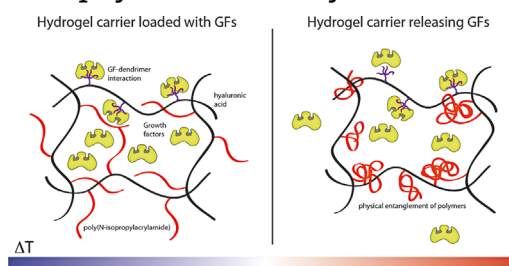


# Injectable Hyaluronan Hydrogels with Peptide-Binding Dendrimers Modulate the Controlled Release of BMP-2 and TGF- $\beta$ 1<sup>a</sup>

Ryan J. Seelbach, Peter Fransen, Daniel Pulido, Matteo D'Este, Fabian Dутtenhoefer, Sebastian Sauerbier, Thomas Freiman, Philipp Niemeyer, Fernando Albericio, Mauro Alini, Miriam Royo, Alvaro Mata, David Eglin\*

BMP-2 and TGF- $\beta$ 1 released from injectable thermoresponsive hydrogels are studied in the presence and absence of branched macromolecules bearing BMP-2 or TGF- $\beta$ 1 affinity binding peptides. The synthesized branched macromolecules and the gelling compositions before and after loading with either BMP-2 or TGF- $\beta$ 1 are characterized physico-chemically and show a significantly lower amount of proteins released in the presence of the affinity binding peptide macromolecules. This study illustrates the potential of affinity binding peptide functionalized dendrimers to modulate the local delivery and availability of growth factors important for musculoskeletal regeneration therapies.



## 1. Introduction

The momentum of research toward ideal biomaterials that deliver growth factors (GFs) foreshadows the roles they will play in the coming future for clinical applications.<sup>[1,2]</sup> Two cytokines, bone morphogenetic protein type 2 (BMP-2) and transforming growth factor beta 1 (TGF- $\beta$ 1),

regulate a variety of processes in the body including tissue growth and development, immune system regulation, and homeostasis.<sup>[3,4]</sup> However, there is much debate about the risks of these drugs,<sup>[5–8]</sup> illustrating the necessity to regiment how they are delivered in the body. The controlled and sustained release of GFs can be administered with biomaterials, for example, by exploiting the

Dr. D. Eglin, R. J. Seelbach, Dr. M. D'Este, Prof. M. Alini  
AO Research Institute Davos, Clavadelerstrasse 8, 7270 Davos  
Platz, Switzerland  
E-mail: david.eglin@aofoundation.org  
R. J. Seelbach  
Universitat de Barcelona, Martí i Franquès 1, 08028 Barcelona, Spain  
Dr. P. Fransen, Prof. F. Albericio  
Institute of Research in Biomedicine, Baldiri Reixac 10-12, 08028  
Barcelona, Spain  
Dr. P. Fransen, Dr. D. Pulido, Prof. F. Albericio, Dr. M. Royo  
Biomedical Research Networking Center in Bioengineering,  
Biomaterials and Nanomedicine, Baldiri Reixac 10-12, 08028  
Barcelona, Spain

Dr. M. Royo  
Combinatorial Chemistry Unit, Barcelona Science Park, Baldiri  
Reixac 10-12, 08028 Barcelona, Spain  
Dr. F. Dутtenhoefer, Dr. S. Sauerbier, Prof. P. Niemeyer  
Universitätsklinik Freiburg, Hugstetter Str. 55, D-79106 Freiburg,  
Germany  
Dr. T. M. Freiman  
Universitätsklinikum Goethe Universität, Schleusenweg 2-16,  
D-60538 Frankfurt am Main, Germany  
Dr. A. Mata  
Queen Mary, University of London, Mile End Road, E14NS London, UK

<sup>a</sup>Supporting Information is available from the Wiley Online Library or from the author.

ability of a polymeric matrix to physically entrap the proteins, or by taking advantage of intrinsic electrostatic affinities of a biocompatible ceramic and the drug.<sup>[9,10]</sup>

Polymer networks swelled in water, or hydrogels, can be loaded with GFs and will serve as depots that deliver a localized and sustained release of the therapeutic agent. Depending on the nature of the chemical structures of the polymers, the timed drug release profile, which is governed by gradient diffusion, will be parametrized by electrostatic interaction and the overall mesh size of the scaffold.<sup>[11–15]</sup> More advanced hydrogel biomaterials feature dynamic functionalities that cause a transitional change of state from liquid to hydrogel upon small environmental perturbations.<sup>[16–20]</sup> These so-called “smart” biomaterials can be administered laparoscopically as a solution, take on the additional role of carrier system, and can serve as vehicles to transport drugs or cells directly to an injury site in a minimally invasive way. Peptide amphiphile solutions that form networks in situ have been shown not only to provide a sustained release of loaded GFs but also to preserve their bioactivity.<sup>[16,17]</sup> Further reports have supported these findings and shown an improved efficacy of BMP-2 for in vivo bone formation.<sup>[21]</sup>

Within this class of delivery systems is a thermosensitive polymer consisting of poly(*N*-isopropylacrylamide)-grafted hyaluronic acid (Hyal-pN) brush copolymers.<sup>[22–24]</sup> This polymer platform is exemplary for its shear-thinning property, injectability, and capacity to form hydrogels with a temperature stimulus, proving its utility to facilitate a sustained drug release.<sup>[24]</sup> Hyaluronan-based hydrogels have been frequently utilized to administer a sustained release of BMP-2 which has been shown to positively influence bone formation.<sup>[11,12,25]</sup> Extended release profiles from hydrogels modified with peptide sequences with selective binding affinity to individual GFs have also been reported.<sup>[16,26]</sup> Interestingly, highly specialized branched macromolecules called dendrimers are monodisperse and globular in shape and have been recently described as effective tools for applications in nanomedicine.<sup>[27–30]</sup> They can be readily modified with versatile terminal sequences to target specific biochemical functions. For example, second-generation PAMAM dendrimers were synthesized

as vectors for doxorubicin and were successfully able to target tumors via the alpha-fetoprotein receptor exhibiting high toxicity even in resistant cell lines.<sup>[31]</sup>

Orthogonal synthesis techniques have been used to synthesize disubstituted dendrimers exhibiting one functionality useful for covalent conjugation while the other four terminal sequences are modified with terminal peptide epitope sequences.<sup>[27–28]</sup> This synthesis technique paved the way for using dendrimers to decorate biomaterials with clusters of peptide epitopes, effectively controlling the molecular architecture of the scaffold microenvironment with nanoscale precision. For instance, multivalent dendrimers exhibiting RGDS peptides that can specifically bind with integrin were covalently grafted to a hyaluronic acid backbone then incorporated into a thermoreversible hyaluronan hydrogel carrier for human mesenchymal stem cells encapsulation.<sup>[30]</sup>

In this study, disubstituted dendrimers bearing one azide functionality and four binding peptides, presenting the *Tyr-Pro-Val-His-Ser-Thr* (YPVHST) or *Leu-Pro-Leu-Gly-Asn-Ser-His* (LPLGNSH) sequences to target BMP-2 or TGF- $\beta$ 1 protein binding, respectively, were synthesized and characterized. These unique macromolecules were then covalently conjugated to hyaluronic acid using a copper-catalyzed azide-alkyne cycloaddition (CuAAC) reaction, mixed with Hyal-pN featuring different lengths of poly(*N*-isopropylacrylamide) (pN), then loaded with BMP-2 or TGF- $\beta$ 1. The influence of the dendrimers and the size of the pN on the in vitro release of loaded BMP-2 and TGF- $\beta$ 1 from the depots were quantified along with the degree of grafting (DG), the peptide contents, and the viscoelasticity of the thermoreversible hydrogels.

## 2. Results

### 2.1. <sup>1</sup>H NMR Characterization

<sup>1</sup>H NMR spectra confirmed the grafting of all the batches of N<sub>3</sub>-pN to the Hyal-pN (Table 1). The DG ratios were calculated in mol% by attributing the ratio of the signal at  $\delta = 1.14$  ppm, corresponding to six protons of the N<sub>3</sub>-pN isopropyl group, to the shift at  $\delta = 3.0$ – $3.8$  ppm,

**Table 1.** Reported  $M_w$  of N<sub>3</sub>-pN and DG and extrapolated size of the Hyal-pN determined by multidetector HPLC and <sup>1</sup>H NMR methodologies.

| Sample | Size of pN [kDa] <sup>a)</sup> | % DG [theory] | % DG [actual] <sup>b)</sup> | Calculated polymer brush size [kDa] |
|--------|--------------------------------|---------------|-----------------------------|-------------------------------------|
| HpN9   | 9.2                            | 4%            | 4.4%                        | 561.0                               |
| HpN16  | 16.3                           | 4%            | 4.4%                        | 767.9                               |
| HpN21  | 21.2                           | 4%            | 4.3%                        | 896.6                               |
| HpN28  | 27.5                           | 4%            | 4.2%                        | 1057.8                              |

<sup>a)</sup>measured by multidetector HPLC; <sup>b)</sup>calculated from <sup>1</sup>H NMR spectrum.

**Table 2.** Reported quantities of peptides and dendrimers per hyaluronic acid disaccharides, extrapolated concentrations within the hydrogel depots, and efficiency of the CuAAC reaction.

| Sample   | Ratio epitope to disaccharide [mmol · mg <sup>-1</sup> ] <sup>a)</sup> | Ratio dendrimer to disaccharide [mmol · mg <sup>-1</sup> ] <sup>a)</sup> | Calculated epitope per hydrogel depot [mM]  | Calculated yield of product |
|----------|--|--|---|-----------------------------|
| Hyal-YPV | $6.5 \times 10^{-6} \pm 1.1 \times 10^{-6}$                            | $1.6 \times 10^{-6} \pm 2.8 \times 10^{-7}$                              | $3.4 \times 10^{-2} \pm 4.1 \times 10^{-3}$ | 33.7 ± 5.7%                 |
| Hyal-LPL | $7.8 \times 10^{-6} \pm 3.0 \times 10^{-7}$                            | $1.9 \times 10^{-6} \pm 7.6 \times 10^{-8}$                              | $4.1 \times 10^{-2} \pm 7.2 \times 10^{-3}$ | 38.9 ± 1.5%                 |

<sup>a)</sup>measured by a. a. analysis.

corresponding to nine protons of the hyaluronic acid disaccharide ring. The calculated DGs of pN were all reported above the theoretical value (Table 1). The higher than expected values can be attributed to the degradation of the hyaluronic acid during CuAAC which would subsequently change the observed ratios of N<sub>3</sub>-pN to Hyal-pa. Direct characterization of the molecular size of the brush copolymers has yet to be made possible due to the difficulty of measuring Hyal-pN with HPLC methods; however, individually, the Hyal-pa and N<sub>3</sub>-pN were characterized with these methods.<sup>[30]</sup> We calculated the theoretical brush copolymer sizes based upon the *M<sub>w</sub>* of the pN batches and the propargylamine substituted hyaluronic acid. Furthermore, the increasing ratio of poly(*N*-isopropylacrylamide) to hyaluronic acid signal is consistent with the grafting of higher molecular weight polymer chains to the polysaccharide backbone. A theoretical size of the brush copolymers was calculated based upon the molecular weight distributions of the Hyal-pa and N<sub>3</sub>-pN, assuming no degradation of the polysaccharide chain (Table 1).

The dendrimer-grafted hyaluronic acid was synthesized based upon the same CuAAC reaction method. However, the theoretical molar ratio of grafted dendrimer to the Hyal-pa backbone was on the order of 10<sup>-5</sup> mol, which was too low for accurate quantification by <sup>1</sup>H NMR. Therefore, the experimental molar ratio was quantified by amino acid analysis.

## 2.2. Amino Acid Analysis of the Dendrimer-Grafted Hyaluronan

Amino acid analysis of the dendrimer-peptide conjugates grafted to Hyal-pa was employed in order to quantify the amount of peptides, and subsequently dendrimers, onto the polysaccharide backbone (Table 2).

## 2.3. Rheological Characterization of the Bicomponent Hydrogel Biomaterials

All Hyal-pN batches showed the temperature sensitive response that is consistent with this polymer system.<sup>[23,30,32]</sup> The concentrations of dendrimers employed in this study did not affect the mechanical properties of the hydrogels which agreed with our previous report (Figure 1).<sup>[30]</sup>

The transition temperatures, the points at which the materials experienced an increase in viscoelasticity, increased along with the size of the pN chains and fell within the range of 27.3–30.1 °C (Figure 1B). The influence of pN size over the viscoelastic moduli at 20 and 37 °C in

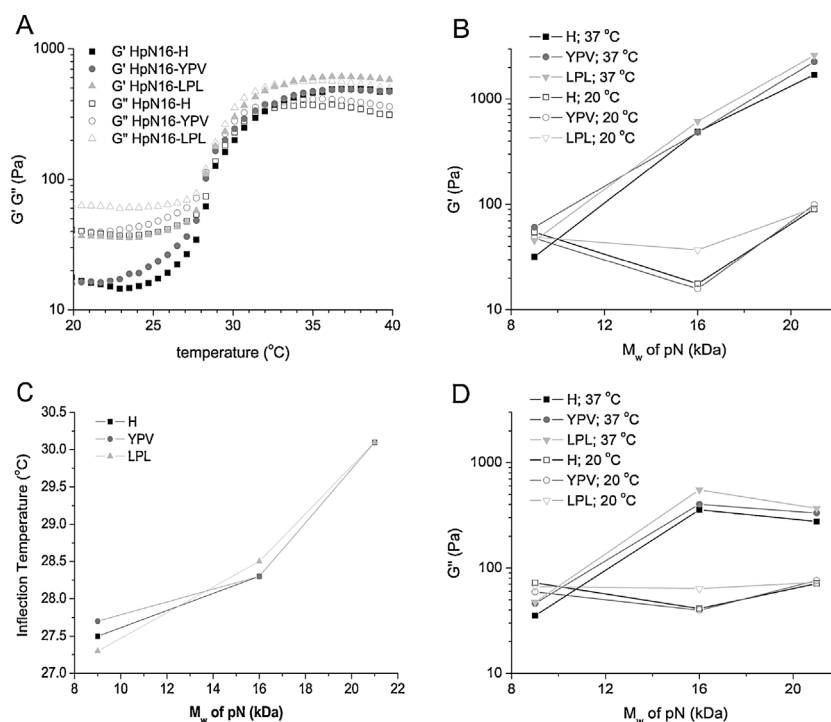


**Figure 1.** Rheological characterization of the bicomponent hydrogels (15% (w/v) in PBS) with (A) the influence of the dendrimer on *G'* and *G''* within HpN16, (B) the influence of pN size on the inflection temperature of the hydrogels, (C) the influence of pN size on *G'* at 37 and 20 °C, (D) and *G''* at the same temperatures. The presence of dendrimers did not influence the mechanical properties in any hydrogels tested.

Figure 1B and 2D highlights the change in rheological properties for the different Hyal-pN batches. For HpN9, there was no temperature driven increase change in either  $G'$  or  $G''$  from 20 to 37 °C (Figure 1B and D). Furthermore, the viscous modulus remained predominant over the storage modulus during the entire temperature sweep. In contrast, HpN16 experienced an increase in both viscous and elastic character. The higher elastic modulus value of 400 Pa compared to the viscous modulus value of 200 Pa at 37 °C indicates the gel state of the aqueous formulation. Furthermore, HpN21 was also a stable hydrogel at 37 °C, exhibiting similar behavior to HpN16, albeit with an even stronger elastic character, with the  $G'$  at 2 kPa and the  $G''$  at 300 Pa.

#### 2.4. In Vitro Release of BMP-2 and TGF- $\beta$ 1 Loaded in Binding Epitope Dendrimer Containing Hydrogels

During the release studies, the stability of the depots was observed. The appearance of cloudy release buffer was a clear indication that a depot was dissolving. The HpN9 hydrogel was not stable and dissolved during the first day of media changes. These data were consistent with results from the rheological experiments, and HpN9 was, therefore, not combined with the dendrimers for the release study. Although HpN16 also slightly disassociated during the first few media changes, most of the depot remained stable and did not further exhibit noticeable changes in volume over the release study period. HpN21 was stable, did not experience any noticeable loss of volume, nor was responsible for the presence of cloudy release media.

We first assessed the in vitro release of the GFs from the three synthesized Hyal-pN batches, at 13% (w/v) in phosphate buffered saline (PBS), and supplemented with Hyal-pa, at 2% (w/v) in PBS (15% (w/v) total polymer) (Figure 2).

For HpN9, most of the measured protein was released within 4 h for both BMP-2 and TGF- $\beta$ 1 as values at 168 h were not significantly different. This is consistent with a soluble formulation rapidly releasing an entrapped molecule. The average amount of GFs released from the non-dendrimer-containing hydrogels

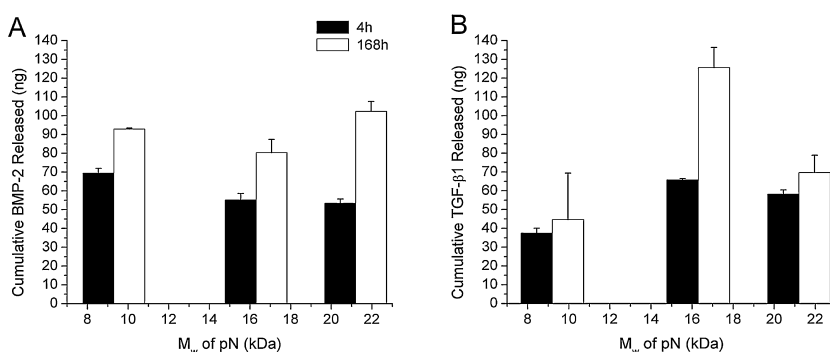


**Figure 2.** Comparison of the cumulative release of (A) BMP-2 and (B) TGF- $\beta$ 1 at 4 h (black) and 168 h (white) from Hyal-pN hydrogels with three  $M_w$  of pN (kDa) and constant DG. The hydrogels were composed of 13% (w/v) Hyal-pN and 2% (w/v) Hyal-pa in PBS.

was  $43.0 \pm 13.8\%$  from all Hyal-pN depots, including HpN9. This pattern indicates that a significant amount of loaded BMP-2 and TGF- $\beta$ 1 interacted with the Hyal-pN macromolecules in vitro. Interestingly, while the amounts of BMP-2 not released were consistent for the three Hyal-pN formulations, more variation are observed for TGF- $\beta$ 1, e.g., HpN16 at 168 h. For the BMP-2 releasing HpN16 and HpN21 depots, the concentrations of BMP-2 released at 168 h were not significantly different to HpN9. A slightly less amount of BMP-2 was found in the release media at 4 h for HpN16

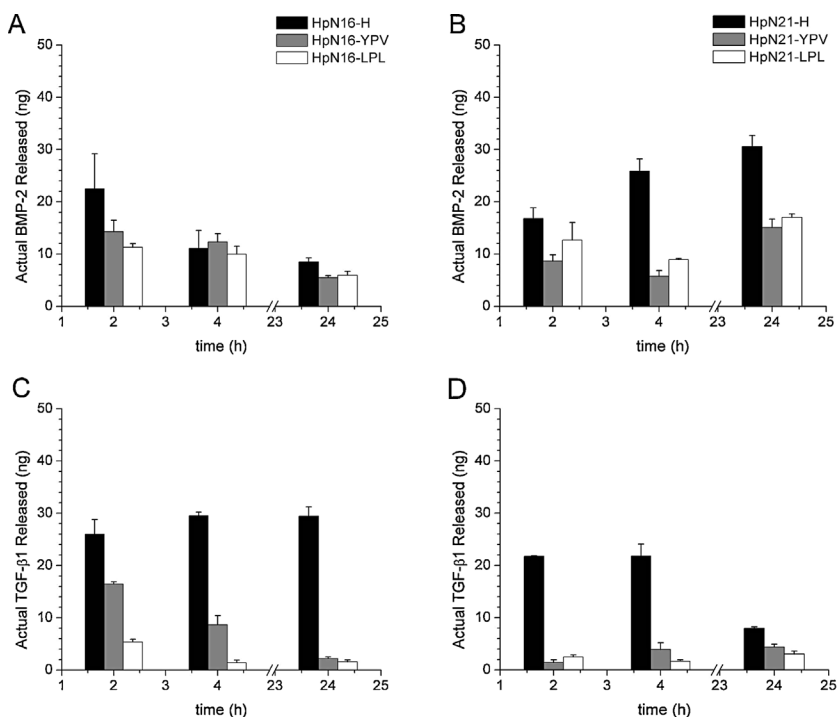


**Figure 3.** Profiles of actual protein released at 2, 4, and 24 h of (A and B) BMP-2 and (C and D) TGF- $\beta$ 1 from (A and C) HpN16 and (B and D) HpN21. Protein release data from the non-dendrimer containing hydrogels are represented in black, whereas the BMP-2 and TGF- $\beta$ 1 binding hydrogels are represented in gray and white, respectively.

and HpN21 compared to HpN9. For the TGF- $\beta$ 1 releasing Hyal-pN, no significant trend in release was found with the pN  $M_w$ .

To assess the effect of the peptide-binding dendrimers on the cytokine release, HpN16 and HpN21 were spiked with Hyal-pa, Hyal-YPV, or Hyal-LPL at 2% (w/v), which corresponded to 0.034 and 0.041 mM concentrations of the BMP-2 and TGF- $\beta$ 1 binding epitopes per hydrogel depot, respectively (Figures 3 and 4).

The profiles of the first 24 h of actual protein released were examined (Figure 3). The difference in release profiles between the unmodified depots of HpN16 and HpN21 and the dendrimer-modified hydrogels was statistically significant according to the Tukey HSD post hoc analysis ( $p < 0.0005$ ). A decrease of BMP-2 and TGF- $\beta$ 1 released in the media was observed when Hyal-YPV and Hyal-LPL were added in the Hyal-pN hydrogel formulation compared to Hyal-pa (no binding epitopes). Statistical analysis verified that the amount of GF released was significantly dependent on the presence of dendrimers and time, regardless of the hydrogel employed,  $F(6,273) = 9.866$ ,  $p < 0.0005$ , partial  $\eta^2 = 0.178$ . The peptide-binding sequences employed in this study, however, were nonspecific to either protein binding

affinity (i.e., TGF- $\beta$ 1 and BMP-2 have similar binding affinities with both LPLGNSH and YPVHST dendrimers). Furthermore, the release profiles between the dendrimer-modified hydrogels were statistically similar according to the Tukey's HSD post hoc analysis ( $p = 0.892$ ).

The long-term cumulative release of GFs from the different Hyal-pN formulations showed similar profiles irrespective of the pN and growth factor type (Figure 4). In the absence of the binding peptides presented via the dendrimers, an initial burst release is followed by a sustained release which reached a plateau after 100 h. The burst release was significantly decreased in the presence of dendrimers, irrespective of the binding epitope. For example, a relatively high amount of BMP-2 was BMP-2, 126 ng, was released from the HpN16 hydrogel depot in absence of dendrimers was measured at one week, whereas only 31 and 29 ng were released within the same time frame for the HpN16-YPV and HpN16-LPL dendrimer containing gels, respectively. The presence of the LPL binding epitope bearing dendrimer resulted in a slightly higher BMP-2 retention in HpN16 compared to the YPV dendrimer, while the inverse was observed in the HpN21. Relatively low amounts of protein were detected (or

released) for HpN21 as well as the dendrimer containing hydrogel counterparts (HpN21-YPV and HpN21-LPL). The LPL dendrimer displayed higher BMP-2 affinity for HpN16 and was only marginally less effective at binding the protein in the case of HpN21.

### 3. Discussion

In order to investigate the role of the density of the physical cross-linking network of Hyal-pN hydrogels, the biomaterials were synthesized with 9, 16, or 21 kDa-sized pN with similar degrees of substitution across all batches. The pN chains typically undergo a transitional hydrophobic collapse upon increasing temperature above the LCST, in effect entangling the polymers into a cohesive material. The  $M_w$  of pN subsequently affects the stability and viscoelastic character of the polymers in PBS. HpN9 showed limited changes in  $G'$  and  $G''$  above 27.5 °C and the  $G'$  never crossed over the  $G''$ . In solution, HpN16 and HpN21 behaved as viscous liquids below their inflection temperatures, with similar  $G''$  values at 20 °C, akin to pristine hyaluronic acid. Whereas above this

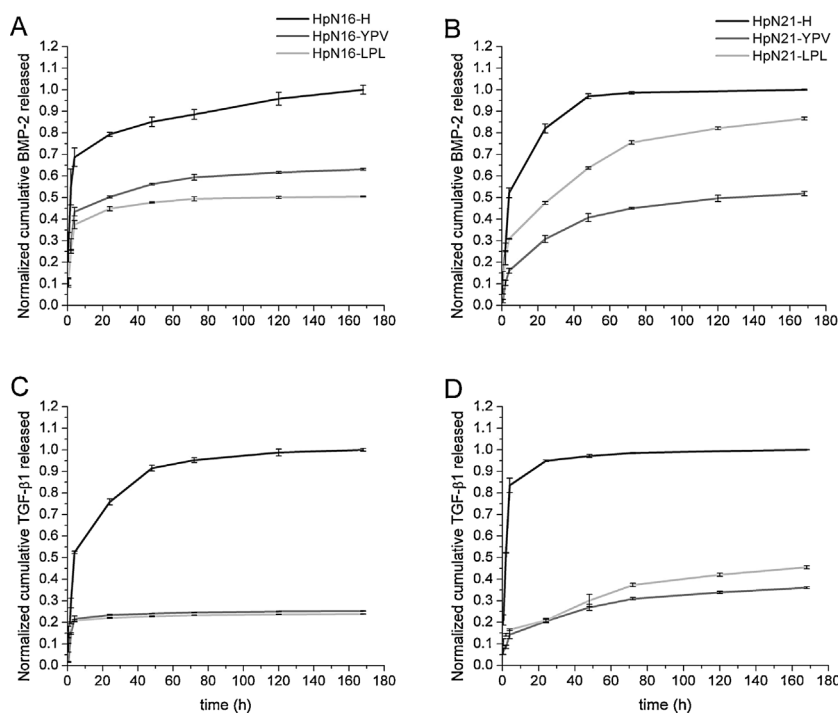


**Figure 4.** Normalized cumulative protein release from loaded hydrogels showing the relative amounts of BMP-2 released from (A) HpN16 and (B) HpN21, and TGF- $\beta$ 1 released from (C) HpN16 and (D) HpN21. The results were normalized to the absolute amount of drug released at one week by the non-dendrimer-containing hydrogels. Protein release data from non-dendrimer-modified hydrogels are represented as a dark gray line, whereas the BMP-2 and TGF- $\beta$ 1-binding hydrogels are represented as gray and light gray lines, respectively.

temperature, the  $G'$  passed over the  $G''$  value indicative of stable hydrogel formation. Furthermore, we observed that within the range of  $M_w$  of pN tested, the materials did not experience significant macroscopic shrinkage. The addition of dendrimers in Hyal-pN did not significantly influence the rheological features. The release profile of BMP-2 and TGF- $\beta$ 1 from the loaded hydrogels initially presented a burst of protein which peaked after 4 h followed by an incremental release thereafter. No significant difference with respect to the size of pN was observed, except for a slight trend showing a diminished release of BMP-2 at 4 h with an increase in size. Additionally, a significant amount of protein could not be measured in the media likely because they were bound to Hyal-pN even in PBS doped with BSA.<sup>[11,13]</sup> This pattern was also true for the HpN9 even though it did not form a stable hydrogel.

The sustained release of drugs from hydrogels depots is governed by several factors including gradient diffusion, non-covalent binding (i.e., Lewis acid–base interactions), physical entrapment (e.g., cross-linking density), and the initial concentration loaded into the system.<sup>[15,13,33]</sup> Thus, the nature of the polymer scaffold is important.<sup>[11,34]</sup> Kim and Valentini hypothesized that the release of BMP-2 from a hyaluronic acid-based hydrogel is attenuated by the electrostatic interaction of negatively charged carboxylic acid groups of the polysaccharide and the primary amine-rich BMP-2, in other words, an acid–base system.<sup>[25]</sup> Only 32% of the total loaded protein was retrieved, whereas 88% was released from a collagen I sponge control. The full observed release of protein from the dendrimer conjugated hyaluronic acid-based hydrogels never reached the amounts delivered from the control hydrogels. It is also possible that the dendrimers delay the release of drugs<sup>[16]</sup> and would deliver a prolonged sustained released over an extended period of time dependent on the degradation of the hyaluronan conjugates. Nevertheless, the inevitable retention of protein within biomaterials has been shown to maintain bioactivity,<sup>[12]</sup> improve cellular invasion,<sup>[35,36]</sup> and increase the deposition of tissue matrix proteins within the scaffolds.<sup>[11,25]</sup> Even extremely low concentrations of BMP-2 localized within a hydrogel are sufficient to program the microenvironment toward guiding cellular differentiation.<sup>[37]</sup> In order to isolate the effects of the dendrimers, the hydrogels with BMP-2 or TGF- $\beta$ 1 were supplemented with 0.1% BSA and 4 mM HCl in order to discourage nonspecific binding with the biomaterial.<sup>[12,13]</sup> The aforementioned peptide-binding sequences were previously identified by phage display.<sup>[16,38,39]</sup> In our case, augmenting the molecular architecture of the drug delivery platform with peptide-binding dendrimers also significantly affected the release of BMP-2 and TGF- $\beta$ 1. In accordance with previous results,<sup>[30]</sup> the influence of dendrimers on the delivery of the cytokines in BSA-supplemented PBS was compared with Hyal-pN containing

Hyal-pa, the precursor of the Hyal-YPV and Hyal-LPL conjugates.

In this study, we demonstrated the ability of the peptide bearing dendrimers to attenuate the protein release from Hyal-pN depots, causing a sharp decrease in the burst phase as well as a lower final concentration at 7 d. The relatively high overall release of protein from the non-dendrimer containing depots compared to compositions modified with dendrimers can be clearly seen for HpN16 and HpN21. We checked the specificity of the synthesized peptide epitopes by performing analogous release studies by loading BMP-2 into depots containing Hyal-LPL (i.e., TGF- $\beta$ 1 binding hyaluronan) peptide, and vice versa. Interestingly, in all scenarios, the dendrimers were at least similarly efficacious in retaining GFs, suggesting that the binding behavior of these peptides are not specific to BMP-2 and TGF- $\beta$ 1 or that the presentation of these peptides on the tip of the dendrimer branched structure render the peptides less specific. Another possibility for the nonspecificity may be due to the fact that the secondary structures of the peptide sequences were randomly oriented since they were not organized within a native protein structure. Hence, binding specificity may stem from the tertiary structure, as is the case with antigenic determinants in antibody recognition. Future studies could more closely examine the peptide dendrimer-binding affinity and specificity employing proteins outside of the TGF superfamily.

## 4. Conclusion

We have designed, developed, and characterized dendrimers which have been augmented with terminal peptide binding sequences and covalently grafted to an injectable hydrogel. The dendrimer-decorated hydrogels attenuated the release BMP-2 and TGF- $\beta$ 1 through affinity-based interactions of the functionalized peptide binding sequences and the GFs. The release studies highlight the potential of incorporating these unique types of dendrimers into a biomaterial platform for musculoskeletal repair.

## 5. Experimental Section

### 5.1. Materials

Hyaluronic acid sodium salt from *Streptococcus equi* was purchased from Contipro Biotech s.r.o. (Czech Republic) ( $M_w = 293$  kDa and  $PD = 1.86$ ). Tetrabutylammonium fluoride trihydrate (TBAF), *N*-dimethylsulfoxide (DMSO), sodium chloride, sodium azide, ascorbic acid sodium salt (NaAsc), copper sulphate pentahydrate ( $\text{CuSO}_4 \cdot 5\text{H}_2\text{O}$ ), ethylenediaminetetraacetic acid disodium salt (EDTA), *N*-isopropylacrylamide (NIPAM), azobisisobutyronitrile (AIBN), *N*-dimethylformamide (DMF), Dowex 50  $\times$  8 cation exchange resin (H type), *N,N'*-diisopropylcarbodiimide (DIPCDI),

trifluoroacetic acid (TFA), *N,N*-diisopropylethylamine (DIEA), triisopropylsilane (TIS), di-*tert*-butyl dianhydride, Zinc, 10 wt% Pd/C, and phosphate buffered saline tablets were purchased from Sigma-Aldrich and were of the purest grade. Spectra/Por-regenerated cellulose dialysis tubing (MWCO = 12–14 kDa) was purchased from Spectrum laboratories. NH<sub>4</sub>Cl was purchased from Pancreac. *O*-(2-Aminoethyl)-*O'*-(2-azidoethyl) pentaethylene glycol (OEG), benzotriazol-1-yl-oxytripyrrolidinophosphonium hexafluorophosphate (PyBOP), and the amino acids used for synthesizing the peptide-binding sequences were purchased from Iris Biotech. Dichloromethane (DCM), methanol (MeOH), hexane, and *tert*-butyl methyl ether were purchased from Solvents Documentation Synthesis. Ethyl (hydroxyimino) cyanoacetate (OxymaPure) was purchased from Luxembourg Industries. Recombinant human bone morphogenetic protein type 2 (BMP-2) and transforming growth factor beta 1 (TGF-β1) were obtained from Medtronic Inc. and Fitzgerald Industries, respectively.

## 5.2. Synthesis of the DTPA Derivative Core Unit: Bn-G1-4Boc

A bifunctional diethylene triamine pentaacetic acid (DTPA)-based core unit **1** was synthesized as described in the literature (Figure S1).<sup>[27]</sup> Molecule **1** (330 mg, 0.47 mmol) was dissolved in 30 mL of 4 M HCl in dioxane and left overnight. The next day, the dioxane was evaporated to yield the unprotected DTPA. The unprotected core was dissolved in 250 mL of DCM/DMF (7:3) and PyBOP (1066 mg, 2.05 mmol) together with BocNH-PEG-NH<sub>2</sub> (873 mg, 2.05 mmol) were added. The basicity of the reaction mixture was adjusted to pH 8 by the addition of DIEA. The reaction was allowed to stir for 2 h after which the solvent was concentrated under reduced pressure. After evaporation of the organic phase, the crude product containing residual DMF was dissolved in 50 mL of DCM and washed three times with 5% NaHCO<sub>3</sub> (50 mL). Another 20 mL of DCM was evaporated after the washing. The crude product redissolved again in 10 mL of DCM and transferred to a 50 mL falcon tube, and then precipitated in 40 mL of hexane followed by vigorous shaking and centrifugation. The supernatant was discarded and the precipitated pellet was purified with flash chromatography over basis alumina oxide with 1% MeOH in DCM as the eluent to yield the desired dendron (**2**, 619 mg, 63%). <sup>1</sup>H NMR (400 MHz, CDCl<sub>3</sub>): δ = 2.65 (m, 4 H), 2.71 (m, 4 H), 3.19 (s, 8 H), 3.25 (m, 8 H), 3.38 (m, 8 H), 3.42 (s, 2 H), 3.48 (m, 16 H), 3.52–3.62 (m, 80 H), 5.08 (s, 2 H), 7.30 (m, 5 H), and 7.70 (bs, NH). <sup>13</sup>C NMR (100 MHz, CDCl<sub>3</sub>): δ = 2.65, 28.36, 52.30, 53.05, 54.97, 58.64, 66.43, 69.61, 69.99, 70.16, 70.40, 78.98, 128.34, 128.39, 128.58, 135.43, 155.98, and 170.80. HPLC: 5 à 100% acetonitrile in water over 8 min (SunFire C<sub>18</sub>), t<sub>R</sub> = 5.98 min. MS: Theoretical mass for [C<sub>97</sub>H<sub>181</sub>N<sub>113</sub>O<sub>38</sub>]<sup>+</sup>: 2 108.2569. Experimental mass detected by LC-MS: 1056.60 (M+2)/2. Experimental mass detected by HRMS: 2 108.2588.

## 5.3. Chemical Coupling of the Dendron with an Azide Terminated Branch: G1-4Boc-1N<sub>3</sub>

The purified dendron (Bn-G1-4Boc, **2**) (800 mg, 0.38 mmol) was dissolved in 20 mL MeOH after which a heterogenous catalyst 10 wt % Pd/C was added (80 mg). The contents were kept under nitrogen and a positive pressure was maintained on the reaction flask using

an H<sub>2</sub>-filled balloon. The reaction was stirred for 2 h after which the flask was purged again with N<sub>2</sub>. The catalyst was removed by filtration over cellite and the filter cake was washed several times with ethyl acetate. The organic phase consisting of MeOH and ethyl acetate was evaporated to yield yellow hued oil. The oil was dissolved in a mixture (7:3) of DCM/DMF (200 mL) and PyBOP (218 mg, 0.42 mmol) together with N<sub>3</sub>-PEG-NH<sub>2</sub> (155 mg, 0.42 mmol) were added. The basicity of the reaction mixture was adjusted to pH 8 by the addition of DIEA. The reaction was allowed to stir for 2 h after which the solvent was concentrated under reduced pressure. After evaporation of the organic phase, the crude product containing residual DMF was dissolved in 50 mL of DCM and washed three times with 5% NaHCO<sub>3</sub> (50 mL). Another 20 mL of DCM was evaporated after the washing. The crude product was redissolved in 10 mL of DCM and transferred to a 50 mL falcon tube then precipitated in 40 mL of hexane followed by vigorous shaking and centrifugation. The supernatant was discarded and the precipitated pellet corresponded to the crude product. The product G1-4Boc-1N<sub>3</sub>, **3**, was purified with flash chromatography over basis alumina oxide and was eluted with 1% MeOH in DCM as the eluent to yield the desired dendron **3** (795 mg, 89%). <sup>1</sup>H NMR (400 MHz, CDCl<sub>3</sub>): δ = 1.44 (s, 36 H), 2.62 (bs, 4 H), 2.69 (bs, 4 H), 3.11 (s, 2 H), 3.21 (s, 10 H), 3.28–3.33 (m, 8 H), 3.39 (t, J = 4.96, 2 H), 3.41–3.47 (m, 10 H), 3.50–3.58 (m, 20 H), 3.58–3.67 (m, 100 H), and 7.57 (bs, NH). <sup>13</sup>C NMR (100 MHz, CDCl<sub>3</sub>): δ = 28.41, 38.93, 40.34, 50.65, 53.19, 58.85, 58.64, 69.61, 70.00, 70.09, 70.20, 70.49, 155.89, and 170.79. HPLC: 5 à 100% acetonitrile in water over 8 min (SunFire C<sub>18</sub>), t<sub>R</sub> = 5.68 min. MS: Theoretical mass for [C<sub>104</sub>H<sub>203</sub>N<sub>15</sub>O<sub>43</sub>]<sup>+</sup>: 2 350.4159. Experimental mass detected by LC-MS: 1 177.74 (M+2)/2. Experimental mass detected by HRMS: 2350.4182.

## 5.4. Solid-Phase Peptide Synthesis of BocNH-YPVHST-OH and BocNH-LPLGNSH-OH

Two peptide sequences Tyr-Pro-Val-His-Ser-Thr (YPVHST) and Leu-Pro-Leu-Gly-Asn-Ser-His (LPLGNSH) were synthesized by solid phase peptide synthesis on a 2-chlorotrityl resin using the Fmoc strategy yielding BocNH-YPVHST-OH and BocNH-LPLGNSH-OH. In both cases, the C-terminal amino acid was introduced onto the solid support by addition of 4 eq. of DIEA onto the resin. The remaining three amino acids were coupled one after the other using OxymaPure and DIPCDI as the coupling reagents using HBTU as the coupling agent and HOBT as the additive in the presence of DIEA and in DMF. After coupling the final amino acid, the N-terminal amino group was capped with the Boc-protecting group by reacting with di-*tert*-butyl dicarbonate and DIEA. The peptides were then cleaved from the resin using mild acidic conditions consisting of short washes with 1% TFA in DCM in order to keep the side chain-protecting groups intact. The cleaved peptides were characterized by HPLC and LC-MS and were found to be 99% pure.

## 5.5. BMP-2-Binding Peptide Biofunctionalization of the Dendrimer Platform: G1-1N<sub>3</sub>-4NH<sub>2</sub>YPVHPST

Dendron **3** (60 mg, 0.025 mmol) was dissolved in 5 mL TFA/H<sub>2</sub>O (95:5) and stirred for 1 h. Subsequently, the TFA was evaporated and the product was precipitated in methyl *tert*-butyl ether. After

decanting the methyl *tert*-butyl ether, the pellet containing the deprotected dendrimer was dissolved in a mixture (7:3) of DCM/DMF (50 mL) and PyBOP (57 mg, 0.11 mmol) together with BocNH-YPVHST-OH (140 mg, 0.11 mmol) were added. The pH was adjusted to 8 by the addition of DIEA. After 2 h, the solvent was concentrated under reduced pressure. After evaporation of the organic phase, the crude product was dissolved in 50 mL of DCM and washed three times with 5% NaHCO<sub>3</sub> (50 mL). Another 20 mL of DCM was evaporated after the washing. The crude product redissolved again in 10 mL of DCM and then precipitated in 40 mL of hexane. The pellet corresponded to the crude product with the side chain-protecting groups of the peptide still intact. The protecting groups were removed by dissolving the pellet in 10 mL of TFA/H<sub>2</sub>O/TIS (95:2.5:2.5). After 1 h, the TFA was removed and the compound was precipitated in cold *tert*-butyl methyl ether to give the crude peptide–dendron conjugate. The crude was then dialyzed overnight using a membrane with MWCO 1 kDa to yield the pure dendron–peptide conjugate (**4**) (57 mg, 45%). **HPLC**: 0 to 100% acetonitrile in water over 8 min (SunFire C<sub>18</sub>), *t<sub>R</sub>* = 3.80 min. **MS**: Theoretical mass for [C<sub>232</sub>H<sub>375</sub>N<sub>51</sub>O<sub>75</sub>]<sup>+</sup>: 5 075.7098. Experimental mass detected by LC-MS: 1 272.04 (M + 4)/4; 1 014.04 (M + 5)/5; 848.25 (M + 6)/6. Experimental mass detected by HRMS: 5 075.7092.

### 5.6. TGF-β1-Binding Peptide Biofunctionalization of the Dendrimer Platform: G1-1N<sub>3</sub>-4NH<sub>2</sub>LPLGNSH

Following the protocol for dendron–peptide conjugate **4**, dendron **3** (90 mg, 0.036 mmol) was deprotected and dissolved in a mixture (7:3) of DCM/DMF (50 mL) and PyBOP (82 mg, 0.158 mmol) together with BocNH-LPLGNSH-OH (215 mg, 0.158 mmol). The synthesized dendron–peptide conjugate **5** (130 mg, 75%) was then purified and characterized as described. **HPLC**: 0 to 100% acetonitrile in water over 8 min (SunFire C<sub>18</sub>), *t<sub>R</sub>* = 3.92 min. **MS**: Theoretical mass for [C<sub>212</sub>H<sub>371</sub>N<sub>55</sub>O<sub>71</sub>]<sup>+</sup>: 4 823.7111. Experimental mass detected by LC-MS: 1 206.64 (M + 4)/4; 967.07 (M + 5)/5; 806.01 (M + 6)/6; 691.08 (M + 7)/7. Experimental mass detected by HRMS: 4 823.7106.

### 5.7. Synthesis of Dendrimer Decorated Hyaluronic Acid

Hydrosoluble hyaluronic acid propargylamide (Hyal-pa) was synthesized based on already established procedures.<sup>[23]</sup> Dendrimer **4** or **5** and Hyal-pa (0.5% w/v) were solubilized in degassed MilliQ water such that the theoretical peptide content was 2 mm, hence 0.5 mm azide concentration, as previously established.<sup>[30]</sup> The CuAAC reaction was initiated by the addition of a solution of CuSO<sub>4</sub> pentahydrate salt and sodium ascorbic acid to the polymer solution such that the final copper to azide molar ratio was equivalent. The reaction was maintained under Schlenk parameters and stirred for 5 h at room temperature while protected from light. The reaction was quenched by the addition of 0.5 g of EDTA disodium salt dehydrate. The yielded polymer products were then dialyzed with 0.1 M NaBr and water and lyophilized until dry. The products were verified by <sup>1</sup>H NMR and the peptide content was quantified by amino acid analysis as previously reported.<sup>[30]</sup> The reaction yield of Hyal-pa modified with dendrimer **4** (Hyal-YPV) was 33.7 ± 5.7%, and with dendrimer **5** (Hyal-LPL) was 38.9 ± 1.5%.

### 5.8. Synthesis of the Thermo-responsive Poly(*N*-Isopropylacrylamide) Derivative of Hyaluronic Acid

The synthesis of four different sizes of azido-terminated poly(*N*-isopropylacrylamide) (N<sub>3</sub>-pN) with *M<sub>n</sub>* equal to 9.3, 16.3, 21.2, and 27.5 × 10<sup>3</sup> g · mol<sup>-1</sup> was performed by RAFT homopolymerization using *S*-1-dodecyl-*S'*-( $\alpha,\alpha'$ -dimethyl- $\alpha''$ -acetic acid) trithiocarbonate as reported.<sup>[40–42]</sup> The molecular weight distributions for N<sub>3</sub>-pN were obtained as previously reported.<sup>[30]</sup> Hyal-pN was synthesized via CuAAC under Schlenk conditions by adding N<sub>3</sub>-pN (9.3, 16.3, 21.2, or 27.5 × 10<sup>3</sup> g · mol<sup>-1</sup>) to 0.5% w/v Hyal-pa in degassed MilliQ water. The N<sub>3</sub>-pN were added to the Hyal-pa solutions such that the final DG would be 4 mol% of the total calculated disaccharides. The degree of pN derivation of the hyaluronic acid was assessed via <sup>1</sup>H NMR spectroscopy (Bruker Avance AV-500 NMR spectrometer) using deuterium oxide as solvent without residual HOD peak suppression and processed with Mestrenova software as already reported.<sup>[43]</sup>

### 5.9. Rheological Characterization of Prepared Hydrogel Compositions

Rheological measurements were performed with an Anton Paar Instruments MCR 302 rheometer equipped with a Peltier plate temperature control and a steel cone geometry,  $\emptyset = 25$  mm, 1°. Samples at room temperature were spread with a spatula onto the Peltier plate preset at 15 °C. Additionally, low viscosity silicon oil was applied along the border of the cone after sample placement in order to avoid evaporation at the solution–atmosphere interface. The Hyal-pN batches synthesized with 9.3, 16.3, 21.2, and 27.5 kDa pN (HpN9, HpN16, HpN21, and HpN28, respectively) were solubilized in PBS at 13% w/v along with the addition of 2% w/v Hyal-pa, Hyal-LPL, or Hyal-YPV (Table 3). Storage modulus (*G'*) and loss modulus (*G''*) were measured as a function of the temperature increase at 1 °C · min<sup>-1</sup> from 20 to 40 °C with 0.1% oscillatory strain at 1 Hz. The linear viscoelastic range was evaluated at 20 and 37 °C by increasing the deformation from 0.01 to 100% strain. Triplicate analysis was performed on each hydrogel.

### 5.10. In Vitro Release of TGF-β1 and BMP-2 from the Hydrogels

All polymer compositions were prepared in PBS at 30% (w/v) and stored at 4 °C under gentle mixing until the materials were fully solubilized (Table 3). Prior to the experiment, 40 mg of the concentrated polymer solutions were weighted in the lids of LoBind Eppendorf tubes. Then, 38 μL of a swelling medium which consisted of 1% BSA in 4 mM HCl (pH 6) was added to the polymer solution. A stock solution of either BMP-2 or TGF-β1 at 100 μg · mL<sup>-1</sup> was delivered into the mixture of solutions such that 200 ng of protein was added to each sample and were left overnight at 4 °C. The following morning, the final depot weights were recorded then incubated at 37 °C for 30 min. Once the hydrogels were fully formed, and confirmed by a quick inversion test, 1 mL of release buffer consisting of 0.1% BSA in PBS was added to the vials. The experiment was carried out at 37 °C under static conditions. Samples were taken at 0.5, 2, 4, 24, 48, 72, 120, and 168 h by fully removing the liquid sample, and replenishing it with fresh release buffer. At the end of

**Table 3.** Description of the hydrogel compositions. All depots contained 13% w/v of their corresponding Hyal-pN batches; additionally 2% w/v of Hyal-pa, Hyal-YPV, or Hyal-LPL was also added to augment the protein binding capability of the biomaterials.

| pN $M_w$ [kDa] <sup>a)</sup> | Non-binding | BMP-2 binding | TGF- $\beta$ 1 binding |
|------------------------------|-------------|---------------|------------------------|
| HpN9                         | HpN9-H      | HpN9-YPV      | HpN9-LPL               |
| HpN16                        | HpN16-H     | HpN16-YPV     | HpN16-LPL              |
| HpN21                        | HpN21-H     | HpN21-YPV     | HpN21-LPL              |
| HpN28                        | HpN28-H     | HpN28-YPV     | HpN28-LPL              |

<sup>a)</sup>measured by multidetector HPLC.

the experiment, depot weights were again recorded after the complete removal of the buffer. The amount of released protein was analyzed with ELISA (R&D Systems, Inc.) following the manufacturer's protocol. In this study, the influence of the following two factors on the release of proteins from the Hyal-pN compositions was assessed: (i) of pN chain length/constant polymer weight and (ii) of the addition of dendrimer-decorated hyaluronan derivatives featuring binding epitopes.

### 5.11. Statistical Analysis of the Release Profiles

A mixed design analysis of variance (ANOVA) was selected as the most appropriate statistical model for analysis of the data. The study framework consisted of repeated measurements taken from the hydrogel depots while comparing the effects of the amount of protein released based upon the type of protein, the type of dendrimer, and the length of pN chains. Studentized residuals generated from the ANOVA procedure were examined and three residuals with a magnitude greater than or equal to  $\pm 3$  standard deviations were determined to be outliers. Analysis of the Q-Q plots generated from the residuals revealed that the data were normally distributed. Statistical significance between groups was determined with the Tukey HSD post hoc test with the significance level set at  $p < 0.05$ .

**Acknowledgements:** The authors would like to thank Markus Glarner for his role in the polymer synthesis of the starting materials Hyal-pa and N<sub>3</sub>-pN. The authors acknowledge the financial support from the AO Foundation (grant number C10-60S). The Spanish Ministry of Economy and Competitiveness (SAF2011-30508-C02-01), the Generalitat de Catalunya (2009SGR 1024), CIBER-BBN (DP) and La Caixa social program (PF) are also acknowledged for their financial support. R.J.S. carried out the experimental design and execution as well as the principal writing of the manuscript. P.F. synthesized the peptide modified dendrimers. D.E. guided R.J.S. during the development and execution of both the experiments and manuscript.

Received: March 9, 2015; Revised: April 10, 2015; Published online: May 5, 2015; DOI: 10.1002/mabi.201500082

**Keywords:** drug delivery; dendrimers; hyaluronan; injectable hydrogels; nanotechnology

- [1] L. Kyllönen, M. D'Este, M. Alini, D. Eglin, *Acta Biomater.* **2015**, *11*, 412.
- [2] M. D'Este, D. Eglin, *Acta Biomater.* **2013**, *9*, 5421.
- [3] C. Bibbo, J. Nelson, D. Ehrlich, B. Rougeux, *Clin. Podiatr. Med. Surg.* **2015**, *32*, 35.
- [4] L. Kubiczakova, L. Sedlarikova, R. Hajek, S. Sevcikova, *J. Transl. Med.* **2012**, *10*, 183.
- [5] E. J. Carragee, E. L. Hurwitz, B. K. Weiner, *Spine* **2011**, *11*, 471.
- [6] M. P. Kelly, J. W. Savage, S. M. Bentzen, W. K. Hsu, S. A. Ellison, P. A. Anderson, *J. Bone Joint Surg. Am.* **2014**, *96*, 1417.
- [7] J. Varga, B. Pasche, *Nat. Rev. Rheumatol.* **2009**, *5*, 200.
- [8] J. T. Buijs, K. R. Stayrook, T. A. Guise, *Cancer Microenviron.* **2011**, *4*, 261.
- [9] K. Lee, E. A. Silva, D. J. Mooney, *J. R. Soc. Interface* **2011**, *8*, 153.
- [10] R. Censi, P. Di Martino, T. Vermonden, W. E. Hennink, *J. Control. Release* **2012**, *161*, 680.
- [11] L. Luca, A.-L. Rougemont, B. H. Walpoth, R. Gurny, O. Jordan, *J. Control. Release* **2010**, *147*, 38.
- [12] Y. Kimura, N. Miyazaki, N. Hayashi, S. Otsuru, K. Tamai, Y. Kaneda, Y. Tabata, *Tissue Eng. A* **2010**, *16*, 1263.
- [13] Y. M. Kolambkar, K. M. Dupont, J. D. Boerckel, N. Huebsch, D. J. Mooney, D. W. Huttmacher, R. E. Guldberg, *Biomaterials* **2011**, *32*, 65.
- [14] S. Gorgieva, V. Kokol, *J. Biomed. Mater. Res. A* **2015**, *103*, 1119.
- [15] F.-M. Chen, Y.-M. Zhao, R. Zhang, T. Jin, H.-H. Sun, Z.-F. Wu, Y. Jin, *J. Control. Release* **2007**, *121*, 81.
- [16] R. N. Shah, N. A. Shah, M. M. Del Rosario Lim, C. Hsieh, G. Nuber, S. I. Stupp, *Proc. Natl. Acad. Sci. USA* **2010**, *107*, 3293.
- [17] H. Hosseinkhani, M. Hosseinkhani, A. Khademhosseini, H. Kobayashi, *J. Control. Release* **2007**, *117*, 380.
- [18] S. Rahimi, E. H. Sarraf, G. K. Wong, K. Takahata, *Biomed. Microdevices* **2011**, *13*, 267.
- [19] S. R. Sershen, S. L. Westcott, N. J. Halas, J. L. West, *J. Biomed. Mater. Res.* **2000**, *51*, 293.
- [20] H. Chen, Y. Gu, Y. Hub, Z. Qian, *PDA J. Pharm. Sci. Technol.* **2007**, *61*, 303.
- [21] O. Jeon, C. Powell, L. D. Solorio, M. D. Krebs, E. Alsberg, *J. Control. Release* **2011**, *154*, 258.
- [22] S. Ohya, H. Sonoda, Y. Nakayama, T. Matsuda, *Biomaterials* **2005**, *26*, 655.
- [23] D. Mortisen, M. Peroglio, M. Alini, D. Eglin, *Biomacromolecules* **2010**, *11*, 1261.
- [24] C. L. Pereira, R. M. Goncalves, M. Peroglio, G. Pattappa, M. D'Este, D. Eglin, M. A. Barbosa, M. Alini, S. Grad, *Biomaterials* **2014**, *35*, 8144.
- [25] H. D. Kim, R. F. Valentini, *J. Biomed. Mater. Res.* **2002**, *59*, 573.
- [26] D. J. Maxwell, B. C. Hicks, S. Parsons, S. E. Sakiyama-Elbert, *Acta Biomater.* **2005**, *1*, 101.

- [27] L. Simon-Gracia, D. Pulido, C. Sevrin, C. Grandfils, F. Albericio, M. Royo, *Org. Biomol. Chem.* **2013**, *11*, 4109.
- [28] D. Pla, M. Martí, J. Farrera-Sinfreu, D. Pulido, A. Francesch, P. Calvo, C. Cuevas, M. Royo, R. Aligué, F. Albericio, M. Álvarez, *Bioconj. Chem.* **2009**; *20*, 1112.
- [29] D. Pulido, F. Albericio, M. Royo, *Org. Lett.* **2014**, *16*, 1318.
- [30] R. L. Seelbach, P. Fransen, M. Peroglio, D. Pulido, P. Lopez-Chicon, F. Duttenhofer, S. Sauerbier, T. Freiman, P. Niemeyer, C. Semino, F. Albericio, M. Alini, M. Royo, A. Mata, D. Eglin, *Acta Biomater.* **2014**, *10*, 4340.
- [31] N. G. Yabbarov, G. A. Posypanova, E. A. Vorontsov, S. I. Obydenny, E. S. Severin, *J. Control. Release* **2013**, *168*, 135.
- [32] M. A. J. Mazumder, S. D. Fitzpatrick, B. Muirhead, H. Sheardown, *J. Biomed. Mater. Res. A* **2012**, *100A*, 1877.
- [33] B. Wen, M. Karl, D. Pendry, D. Shafer, M. Freilich, L. Kuhn, *J. Biomed. Mater. Res. B Appl. Biomater.* **2011**, *97B*, 315.
- [34] H.-G. Xie, X.-X. Li, G.-J. Lv, W.-Y. Xie, J. Zhu, T. Luxbacher, R. Ma, X.-J. Ma, *J. Biomed. Mater. Res. A* **2010**, *92A*, 1357.
- [35] A. K. Ekaputra, G. D. Prestwich, S. M. Cool, D. W. Huttmacher, *Biomacromolecules* **2008**, *9*, 2097.
- [36] A. K. Ekaputra, G. D. Prestwich, S. M. Cool, D. W. Huttmacher, *Biomaterials* **2011**, *32*, 8108.
- [37] J. Xu, X. Li, J. B. Lian, D. C. Ayers, J. Song, *J. Orth. Res.* **2009**, *27*, 1306.
- [38] T. Boonthekul, D. J. Mooney, *Curr. Opin. Biotechnol.* **2003**, *14*, 559.
- [39] H. A. Behanna, J. J. M. Donners, A. C. Gordon, S. I. Stupp, *J. Am. Chem. Soc.* **2005**, *127*, 1193.
- [40] M. Li, P. De, S. R. Gondi, B. S. Sumerlin, *Macromol. Rapid Commun.* **2008**, *29*, 1172.
- [41] S. R. Gondi, A. P. Vogt, B. S. Sumerlin, *Macromolecules* **2007**, *40*, 474.
- [42] M. H. M. Oudshoorn, R. Rissmann, J. A. Bouwstra, W. E. Hennink, *Polymer* **2007**, *48*, 1915.
- [43] M. D'Este, M. Alini, D. Eglin, *Carbohydr. Polym.* **2012**, *90*, 1378.